INVESTIGATION OF HEAT TRANSFER ENHANCEMENT BY USING AL_2O_3/WATER NANOFLUID IN RECTANGULAR CORRUGATED CHANNEL

Nehir Tokgoz[1*], Veli Ozbolat[2] , Besir Sahin[2]

[1]Department of Energy Systems Engineering, Osmaniye Korkut Ata University, Osmaniye, Turkey
[2]Department of Mechanical Engineering, Cukurova University, Adana, Turkey

ABSTRACT: In this study, effects of water-based Al_2O_3 nanofluids on flow characterictisc and heat transfer enhancement in rectangular corrugated channels are investigated numerically. Flow between two isothermally walls is assumed to be two-dimensional, fully developed and laminar. Phase angle effects were investigated with varying the phase angle from 180 to 0 while keeping the corrugated wall geometries fixed. Governing, momentum and energy equations are numerically solved using finite volume method based on SIMPLE algorithm. Simulations are performed for nanoparticle volume fractions between 0 to 0.08 and Reynolds number ranging from 500 to 2000. Numerical results are compared with results obtained from literature and they are in close agreement with each other. Effects of phase angle, nanoparticle volume fraction and Reynolds number on Nusselt number, friction factor and thermal performance factor are investigated.

Keywords: Corrugated channels, heat transfer enhancement, nanofluid

Dikdörtgen Oyuklu Kanalda Al_2O_3 nanoakışkanıyla Isı Transferinin İyileştirilmesinin İncelenmesi

ÖZET: Bu çalışmada, içerisinde dikdörtgen kesitli oyukların bulunduğu kanal akışında, nano parcacıkların (AL_2O_3-su) akış karakteristikleri ve ısı transferini iyileştirme üzerine etkileri sayısal olarak incelenmiştir. Kanal duvarları izotermal, akış iki boyutlu, tam gelişmiş ve laminer kabul edilmiştir. Dikdörtgen kesitli oyukların geometrik özellikleri ve cidarlar arasındaki boşluklar sabit tutularak faz açıları 180^o ile 0^o arasında değiştirilerek akış üzerine etkisi incelenmiştir. Yapılan analizlerde sonlu hacimler yöntemi kullanarak yönetici denklemler, momentum ve enerji eşitlikleri SIMPLE algoritması kullanarak çözümlenmiştir. Analizler Al_2O_3 nanoakışkanının farklı nanopartikül hacimsel oranları, $0 \leq \phi \leq 0.08$ için gerçekleştirilmiştir. Çalışma $500 \leq Re \leq 2000$ aralığında yapılarak elde edilen sonuçlar daha önce literatürde yapılan çalışmalarla mukayese edilmiş, sonuçların uyumlu olduğu gözlemlenmiştir. Faz açısının, parçacık hacimsel oranının ve Reynolds sayısının Nusselt sayısı, Nu, sürtünme faktörü,f ve ısı transferi iyileştirme faktörü, η üzerine etkisi incelenmiştir.

Anahtar Kelimeler: Oyuklu kanallar, ısı transferinin iyileştirilmesi, nanoakışkan

1. INTRODUCTION

Heat exchanger efficiency which can be increased by improving heat transfer enhancement has recently become more important in many applications. One way to increase heat transfer enhancement of heat exchangers is to use optimum channel geometry which do not bring much pressure loss. Corrugated channels are used in a wide array of heat transfer applications because they are easy to fabricate, increase compactness and can be used to increase the heat transfer rate if implemented in an appropriate Reynolds number regime. Corrugated channels do not have significant effects if operated in steady regime but they are very effective on heat transfer enhancement when the flow is unsteady since interactions between boundary layer and core fluid are improved as observed experimentally and numerically [1-3]. Corrugated walls in heat exchangers develop the recirculation region near the corrugations and increase mixing of the fluid which leads heat transfer enhancement. However, increasing the flow mixing causes higher pressure drop. In addition, corrugated walls increase heat transfer enhancement by breaking and destabilizing the thermal boundary layer. In the literature, flow characteristics and heat transfer performance of conventional fluids in the corrugated channels have been studied experimentally and numerically. Goldstein and Sparrow [4] were the first to study the local heat and mass transfer characteristics of wavy wall channels. Two corrugated waves were used for laminar, transitional, and low Reynolds number turbulent flow regimes. They concluded that corrugated wall has a negligible effect on heat transfer rate in the laminar flow regime. However, heat transfer rates were improved by a factor of three over those of conventional straight channel. Desrues et al. [5]

*Corresponding Author: Nehir TOKGOZ, nehirtokgoz@osmaniye.edu.tr

investigated the pressure drop and heat transfer enhancement of ribbed channel for several Reynolds number. They found that heat transfer enhances only when Re is greater than a critical value, while pressure drop increases monotonically with Re. Similar study was made by Eiamsa-ard and Promvonge [6]. They studied turbulent forced convection in a two-dimensional channel with periodic transverse grooves on the lower channel wall for Reynolds number ranging from 6000 to 18000. It is found that the grooved channel increases heat transfer up to 158% over the smooth channel. Yin et al. [7] numerically studied the flow characteristics and heat transfer in sinusoidal corrugated channel for different phase shift. Air was selected as a working fluid and the simulations were performed for a Reynolds number range of 2000 to 10000. Their results showed that the corrugated channels have a significant heat transfer enhancement with increased pressure loss, and phase shift effects are more seen in higher Re region than lower. Due to poor thermal conductivity, heat exchangers of conventional fluids such as water, air, oil shows low performance. With the inclusion of metalic or non-metalic particles with nano-scale sizes within conventional fluids, thermal conductivity of these fluids brings significant heat transfer resulting in greater heat exchanger efficiency. Masuda et al. [8] and Choi et al. [9] were the first to investigate nano-fluids. Choi et al. [10] showed that thermal conductivity of the fluid increased up to two folds using nanoparticles below 1% concentration. Masuda et al. [8], and Xuan and Li [11] revealed that addition of nanoparticles within concentration range of 1-5% increased thermal conductivity more than 20 %. Eastman et al. [12] showed that adding 5% nano-crystalline copper oxide particles into water increases thermal conductivity of water approximately 60%. Santra et al. [13] studied heat transfer in two dimensional horizontal duct for a Reynolds number ranging from 5 to 1500 and nanoparticle volume fraction from 0 to 0.05. It is indicated that heat transfer increases with increase in Reynolds number and nanoparticle volume fraction. Heidary and Kermani [14] numerically studied heat transfer enhancement and fluid flow in a sinusoidal wall channel with copper-water nano-fluid. Their results revealed that integrating wavy wall and adding nanoparticle within base fluid could increase heat transfer by 50%. Ahmed and his coworkers [15, 16] studied heat transfer and pressure drop of copper-water nano-fluid through corrugated channel. As the nanoparticle volume fraction and Reynolds number increase, significant increase in Nusselt number and slight increase in pressure drop was observed.

To our knowledge no paper in the literature has so far studied heat transfer in corrugated wall channels with nanofluid for different phase shifts. Therefore, the present study aims to investigate the effects of phase shift, nanoparticle volume fraction and Reynolds number on heat transfer and flow behavior. Numerical method is employed for flow in channels having rectangular corrugated plates with three different phase shifts, 180°, 90°, and 0° under constant wall temperatures with nanoparticle volume fraction range of 0-0.08 and Reynolds number ranging from 500 to 2000.

2. MATERIAL AND METOD

2.1. Problem Description and Numerical Method

In the present study, 180°, 90°, and 0° phase arrangements namely case 1 (C_1), case 2 (C_2), and case 3 (C_3), respectively, are investigated for rectangular corrugated channels. Figure 1 shows two-dimensional channels consist of two rectangular corrugated plates with amplitude of (a) and corrugation length of (S).

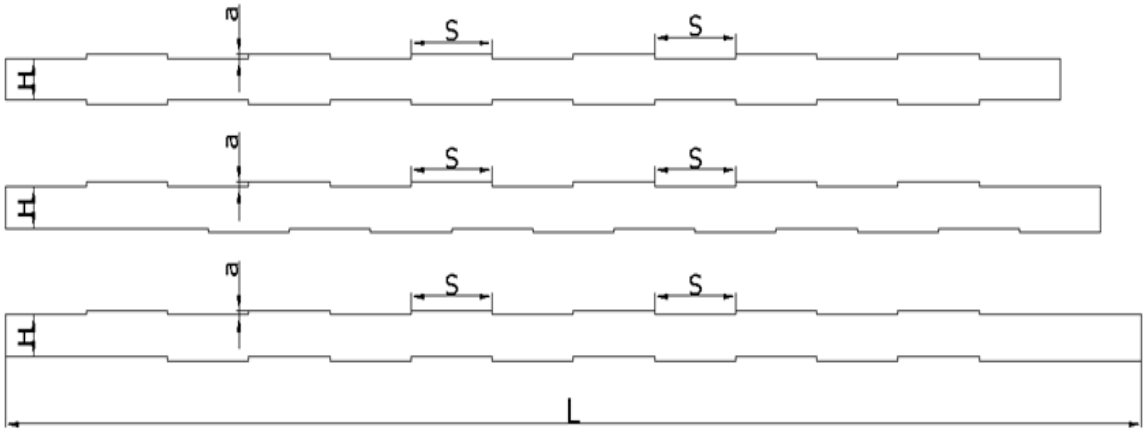

Figure 1. Schematic diagram of the corrugated channels studied

The width of the channel is very large compared to the height. All the cases have constant relative amplitude of a/H=0.3. The uniform temperature of the fluid at the inlet face is taken less than that of corrugated walls. The

flow is taken Newtonian, two-dimensional and

incompressible. The nanofluid which is modeled as a single-phase flow [17-19] is a mixture of water and uniform size and shape of solid spherical alumina particles. Nanoparticle size of 25nm is used for water-alumina flow. The numerical simulations are performed over a range of Reynolds number, Re, 500≤Re≤2000 and nanoparticle volume concentrations, ϕ ,2%≤ ϕ ≤ 8%. Non-conformal grid system is defined for each case. Grids are finer near the boundaries while coarser at the core region as seen in Figure 2.

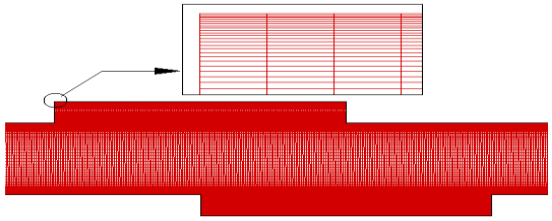

Figure 2. A sample of grid configuration used for 90° phase angle

Problems are computed using the governing equations under steady condition. Standard k-ε is carried out for prediction of the turbulence characteristics. This code uses Finite Volume method for discretizing the governing equations of flow and SIMPLE algorithm proposed by Patankar [20] for resolving the pressure-velocity coupling system. As the convergence criterion, 10^{-8} was chosen for all parameters in computational domain.

2.2. Boundary Conditions and Governing Equations

Figure 3 demonstrates the applied boundary conditions in the present study. Constant temperature and no slip condition are defined for lower and upper walls of the channels. Input fluid has uniform temperature distribution at the inlet. Most of the applications, flow before the heat exchanger is in fully developed condition.

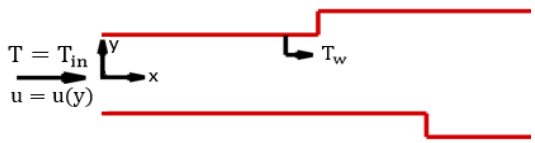

Figure 3. Applied boundary conditions

Since the flow requires higher upstream length to become fully developed, fully developed velocity profile is defined at the inlet section for avoiding extra time and computational efforts. The mathematical descriptions of the boundary conditions are

At inlet section

$$u_{in} = 6\bar{u}\left[0.25 - \left(\frac{y}{H}\right)^2\right] \quad and \quad T = T_{in} \tag{1}$$

On the channel walls

$$u = v = w = 0 \quad and \quad T = T_w \tag{2}$$

On the channel axis

$$\frac{\partial \bar{u}}{\partial y} = \frac{\partial \bar{v}}{\partial y} = \frac{\partial \bar{w}}{\partial y} = \frac{\partial \bar{T}}{\partial y} \tag{3}$$

Calculations for a range of Reynolds number, 500≤Re≤2000 are performed from

$$\mathrm{Re} = \frac{\rho_f \bar{u} D_h}{\mu_f} \tag{4}$$

where

$$D_h = 2H \tag{5}$$

The continuity, momentum and energy equations can be expressed, respectively, as:

$$\frac{\partial}{\partial x_i}(\rho u_i) = 0 \tag{6}$$

$$\frac{\partial}{\partial x_i}\left(\rho u_i u_j\right) = -\frac{\partial p}{\partial x} + \frac{\partial}{\partial x_j}\left[\mu\left(\frac{\partial u_i}{\partial x_j} + \frac{\partial u_j}{\partial x_i}\right)\right] + \frac{\partial}{\partial x_j}\left(-\rho\overline{u_i' u_j'}\right) \tag{7}$$

$$\frac{\partial}{\partial x_i}\left(\rho u_i T\right) = \frac{\partial}{\partial x_j}\left[\left(\Gamma + \Gamma_t\right)\frac{\partial T}{\partial x_j}\right] \tag{8}$$

The molecular thermal diffusivity and turbulent thermal diffusivity are defined as

$$\Gamma = \frac{\mu}{\mathrm{Pr}} \quad and \quad \Gamma_t = \frac{\mu_t}{\mathrm{Pr}_t} \tag{9}$$

The last term of the momentum equation is called the Reynolds stresses. The Reynolds stresses are commonly modeled using the Boussinesq hypothesis in order to relate the Reynolds stresses to the mean velocity gradients. This relation is defined as

$$-\rho\overline{u_i' u_j'} = \mu_t\left(\frac{\partial u_i}{\partial x_j} + \frac{\partial u_j}{\partial x_i}\right) = \tau_{ij} \tag{10}$$

The turbulent or eddy viscosity with respect to applied turbulence model is

$$\mu_t = \rho C_\mu \frac{k^2}{\varepsilon} \tag{11}$$

The turbulent kinetic energy and the rate of turbulent kinetic energy dissipation are defined, respectively, as [21]:

$$\frac{\partial}{\partial x_i}(\rho k u_i) = \frac{\partial}{\partial x_j}\left[\left(\mu + \frac{\mu_t}{\sigma_k}\right)\frac{\partial k}{\partial x_j}\right] + G_k - \rho\varepsilon \quad (12)$$

$$\frac{\partial}{\partial x_i}(\rho \varepsilon u_i) = \frac{\partial}{\partial x_j}\left[\left(\mu + \frac{\mu_t}{\sigma_\varepsilon}\right)\frac{\partial \varepsilon}{\partial x_j}\right] + C_{\varepsilon 1}\frac{\varepsilon}{k}G_k - C_{\varepsilon 2}\rho\frac{\varepsilon^2}{k} \quad (13)$$

where the rate of turbulent kinetic energy generation is [21]

$$G_k = -\rho\overline{u_i' u_j'}\frac{\partial u_j}{\partial x_i} \quad (14)$$

The closure coefficients are given by

$$C_{\varepsilon 1} = 1.44, \quad C_{\varepsilon 2} = 1.92, \quad C_\mu = 0.09, \quad \sigma_k = 1.0$$

Density and heat capacity of the nanofluid are calculated from water and the nanoparticle properties at the reference temperature. The effective density and heat capacity of the nanofluid are determined from:

$$\rho_{nf} = (1-\phi)\rho_{bf} + \phi\rho_{np} \quad (15)$$

$$(\rho C_p)_{nf} = (1-\phi)(\rho C_p)_{bf} + \phi(\rho C_p)_{np} \quad (16)$$

The dynamic viscosity

$$\mu_{nf} = \frac{\mu_{bf}}{(1-\phi)^{2.5}} \quad (17)$$

Effective conductivity

In this study, conductivity of nanofluid is estimated by using the model proposed by Vajjha and Das [22] which considers both static dilute suspension and Brownian motion of the nanoparticles.

$$k_{nf} = k_{Static} + k_{Brownian} \quad (18)$$

The value of K_{static} can be calculated using the Maxwell-Garnett's model

$$k_{Static} = \frac{k_{np} + 2k_{bf} - 2(k_{bf} - k_{np})\phi}{k_{np} + 2k_{bf} + (k_{bf} - k_{np})\phi}k \quad (19)$$

Brownian term in Eq. (18) is computed using the following equation

$$k_{Brownian} = 5x10^4\ \beta\ \phi\ \rho_{bf}\ C_{p\,bf}\ \sqrt{\frac{\kappa T}{\rho_{np} d_{np}}} \quad (20)$$

$f(T,\phi)$

where

$$f(T,\phi) = (2.8217x10^{-2}\phi + 3.917x10^{-3})(\frac{T}{T_0}) + (-3.0669x10^{-2}\phi - 3.91123x10^{-3}) \quad (21)$$

$$\beta = 8.4407(100\,\phi)^{-1.07304} \quad 1\% \le \phi \le 10\% \quad and \quad 298K \le T \le 363K \quad (22)$$

Physical properties of nanoparticle are indicated in Table 2.

Table 2. Physical properties of Al_2O_3 nanoparticle

ρ (kg/m^3)	**K (w/(m.k))**	**Cp (J/(kg.K))**
3890	35	880

The surface heat transfer coefficient is estimated using the following equation

$$h(x) = \frac{q''(x)}{T_w - T_m} \quad (23)$$

where T_m, is bulk temperature which can be determined as [23]

$$T_m = \frac{\int_0^{H/2} uTdA}{\int_0^{H/2} udA} \quad (24)$$

In addition, the value of the local Nusselt number is computed using the following correlation

$$Nu = \frac{hD_h}{k} \quad (25)$$

Furthermore, the value of the mean Nusselt number is obtained by integration of Eq. (25) over the corrugated duct surface as

$$\overline{Nu} = \frac{1}{\xi}\int_0^{\xi} Nu dx \quad (26)$$

Where

$$\xi = \sum_{i=0}^{i=n}(p_i + S_i) \quad (27)$$

The value of the Colburn factor is predicted by

$$j = \frac{\overline{Nu}}{\mathrm{Re}.\mathrm{Pr}^{1/3}} \quad (28)$$

The friction factor is calculated from

$$f = \Delta p \frac{2D_h}{L\left(\rho\overline{u}^{-2}\right)} \quad (29)$$

2.2. Grid independence test and validation of numerical methods

For the corrugated channel the grid independency test was performed with two grid sizes for C_1, C_2, and C_3. The first grid system has the minimum element size of 0.0005 and the finer grid system has the minimum element size of 0.0004 near the duct wall. Details of grid systems are given in Table. 1.

Table 1. Details of applied grids for grid size independence study

Case title	Phase Arrangement	Minimum element size	Grid number
Present case	C1	0.0005	290826
	C2	0.0005	305608
	C3	0.0005	314670
Finer grid case	C1	0.0004	356415
	C2	0.0004	369930
	C3	0.0004	374457

The local Nusselt number and friction factor for three geometries are shown in Figure 4.
It is observed that the values of Nusselt number and friction factor obtained at different grid size change by less than 1%. Thus, the minimum element size of 0.0005 grids can adequately resolve the problem and is used throughout this study.

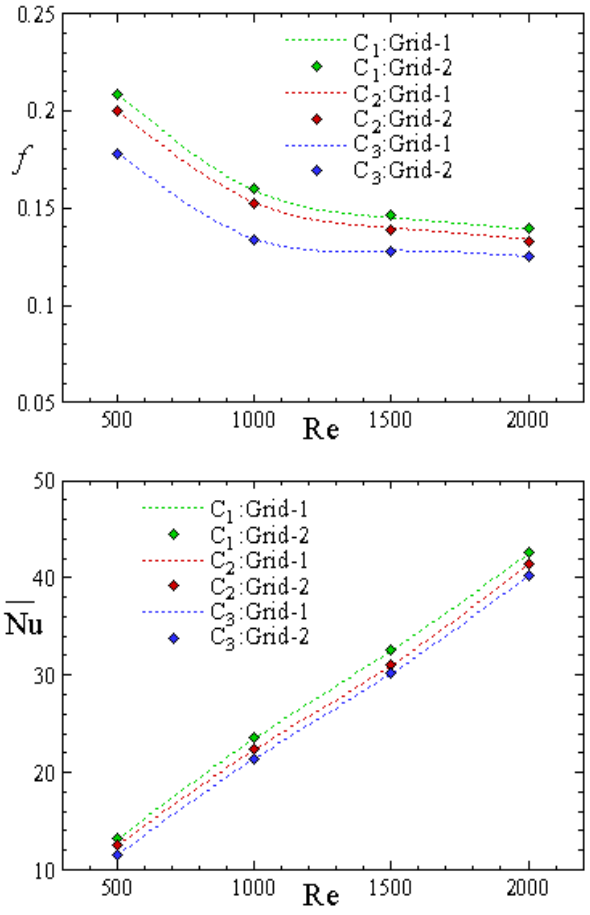

Figure 4. Variation of friction factor and Nusselt number for different grid sizes.

To validate the numerical predictions, the thermal-hydraulic characteristics are computed for plain duct using different Reynolds numbers and are compared with previous works [23, 24]. Figure 5 demonstrates the variations over the friction factor and Colburn factor as functions of the Reynolds number. Here, the predicted results for the friction factor are compared with analytic solution [23] while the values of the Colburn factor are compared with the previous study presented in Shah and London [24]. It is observed that the predicted thermal-hydraulic characteristics match with previous analytics results.

3. RESULTS AND DISCUSSION

3.1.Geometry Effects

In order to see the effects of channel phase shift on the thermal-hydraulic characteristics, water flow in three geometries are studied and obtained results are compared with that of plain duct. Figure 6 shows the effects of channel phase shift on the variation of streamwise velocity and turbulent intensity at the axis for Reynolds number ranging from 500 to 2000.
It is observable that using rectangular corrugated plates develops harmonic velocity distribution on the axis of the channel. The amplitude of the velocity distribution depends on the phase angle and the Reynolds number.
The amplitude of the streamwise velocity distribution increases with Reynolds number. In addition, highest amplitude occurs at 180°. Corrugated plates lead turbulence on the axis of the channel. Turbulence intensity rate varies with Reynolds number and phase angle. For all the geometric configurations, the rate of turbulence intensity increases with Reynolds number as it can be seen from Figure 6 (right). Increasing the flow mixing improves the thermal transport however increase in flow mixing causes more pressure drop. Figure 7 shows the friction factor vs. Reynolds number for different plate configurations.
It can be seen that friction factor decreases with increase in Reynolds number for all the configurations. In addition, using corrugated plates produces more friction compare to the plain duct. The friction difference between corrugated ducts and plain duct is very small at low Reynolds numbers and it increases with Reynolds number. Moreover, the friction factor increases with phase angle and case 1 (C_1) has highest friction factor values for all Reynolds number studied.
Figure 8 depicts the variation of the average Nusselt with Reynolds number for different plate configurations. Since the flow mixing increases with using plate corrugations, the rate of heat transfer and the thermal efficiency for three cases are higher than those of the plain duct. The heat transfer enhancement increases with Reynolds number and phase angle. It is found that minimum Nusselt number enhancement for corrugated plate channels over the plain duct are 1.2, 1.14, and 1.05 for C_1, C_2, and C_3 respectively. At Re=2000, on the other hand, Nusselt number enhancements reach their

maximum value at 2.69, 2.62, and 2.54 for C_1, C_2, and C_3, respectively.

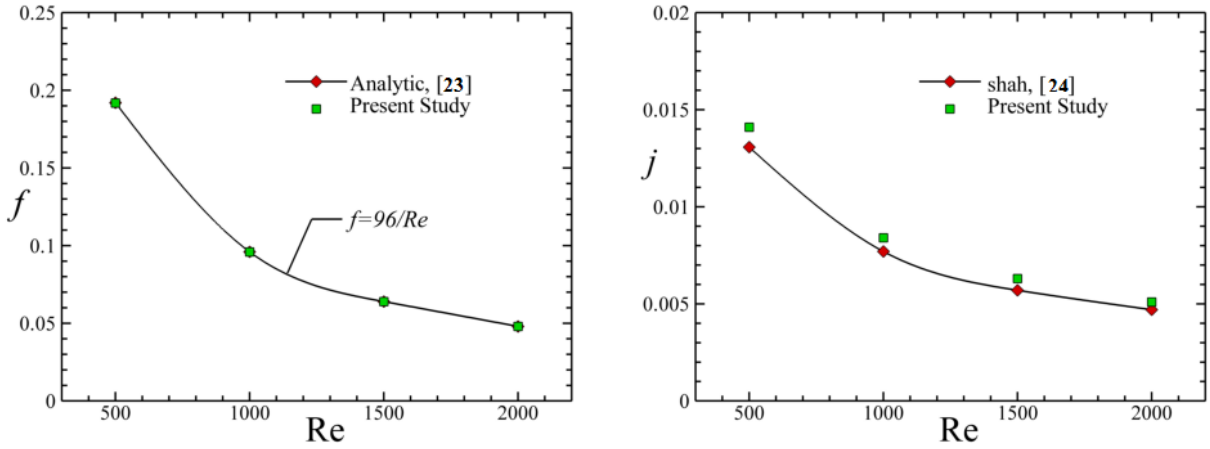

Figure 5. Comparisons of the friction factors of the present study and analytical results and Colburn factors obtained from the present computation and those of shah [24]

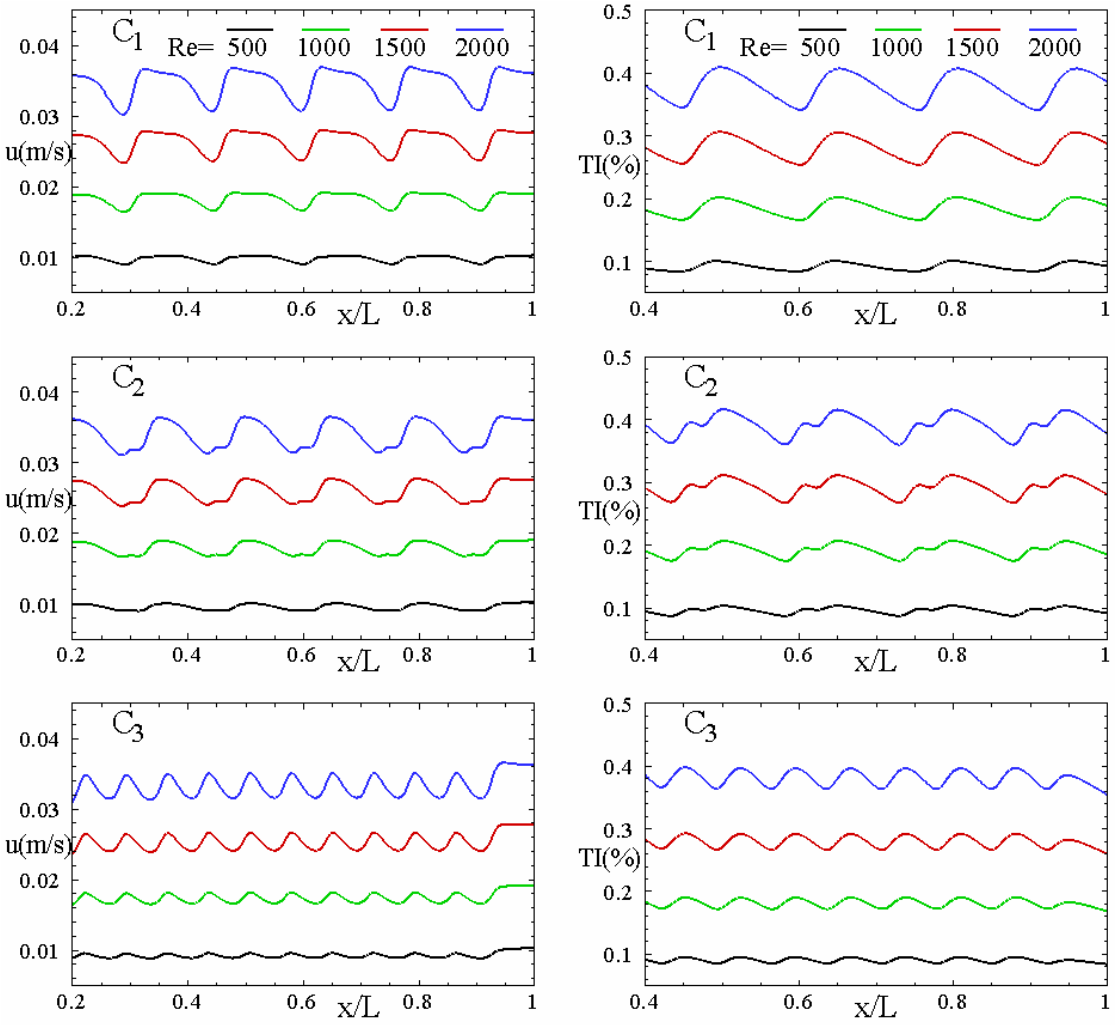

Figure 6. Distribution of streamwise velocity and turbulence intensity along the channel axis

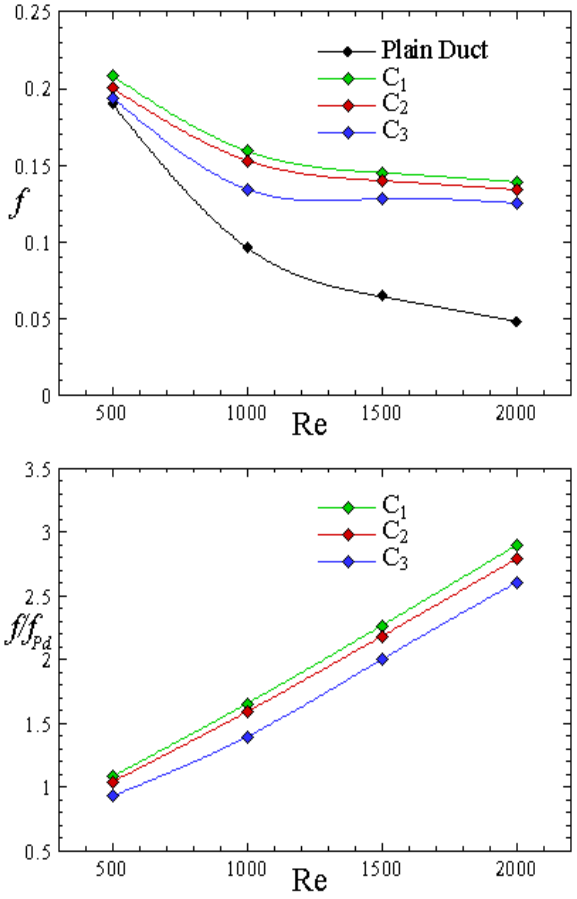

Figure 7. Variation of friction factor with the Reynolds number for plain duct, C1, C2, and C3 and comparison with plain duct.

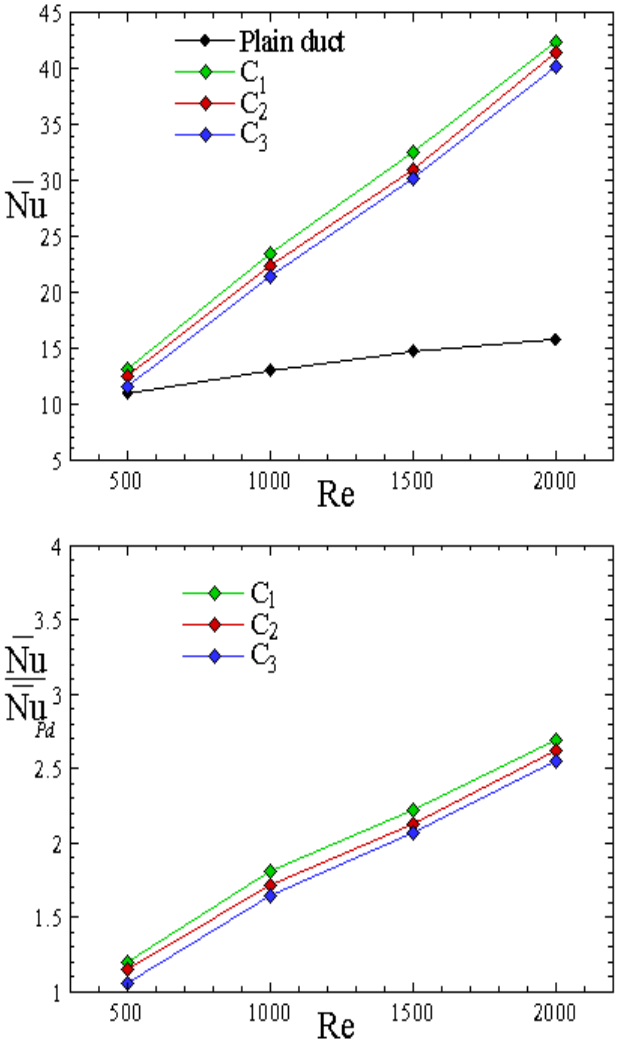

Figure 8. Variation of the Nusselt number with the Reynolds for plain duct, C_1, C_2, and C_3 and comparison with plain duct

3.2.Nanofluid Effects

Heat transfer and flow behavior of nanofluid flow in channel with rectangular corrugations for different phase angles and Reynolds numbers are presented and obtained results are compared with those of water flow. Figure 9 gives the friction factor variations with Reynolds number for all the configurations and nanoparticle volume fractions.

It can be seen that friction factor increases with solid fraction for all the phase angles since nanofluid viscosity and Brownian motion of nanoparticles increase with nanoparticle volume fraction. Effects of nanafluid flow on the thermal characteristics of corrugated channels are shown in Figure 10. The average Nusselt number increases with nanoparticle volume fraction and Reynolds number. Brownian motion of nanoparticles increasing thermal energy transport provides additional heat transfer enhancement. The highest enhancements in Nusselt number are found at Reynolds number of 500 and nanoparticle volume fraction of 8%, with an enhancement of 20%, 22.7%, and 21.2% over the water flow for C_1, C_2, and C_3 respectively. Since using nanofluids in corrugated channels increases both Nusselt number and friction factor, efficiency index of flow should be calculated to find the optimum case. Figure 11 illustrates the efficiency index variation with Reynolds number for different nanoparticle volume fractions and phase angles.

It is seen that efficiency index increases with nanoparticle volume fraction. On the other hand, the efficiency index decreases slightly with Reynolds number. Among all cases, efficiency index of C_2 has highest value. The maximum efficiency index enhancements are 12.2%, 13.4%, and 12.9 for C_1, C_2, and C_3 respectively at Reynolds number of 500 and nanoparticle volume fraction of 8%.

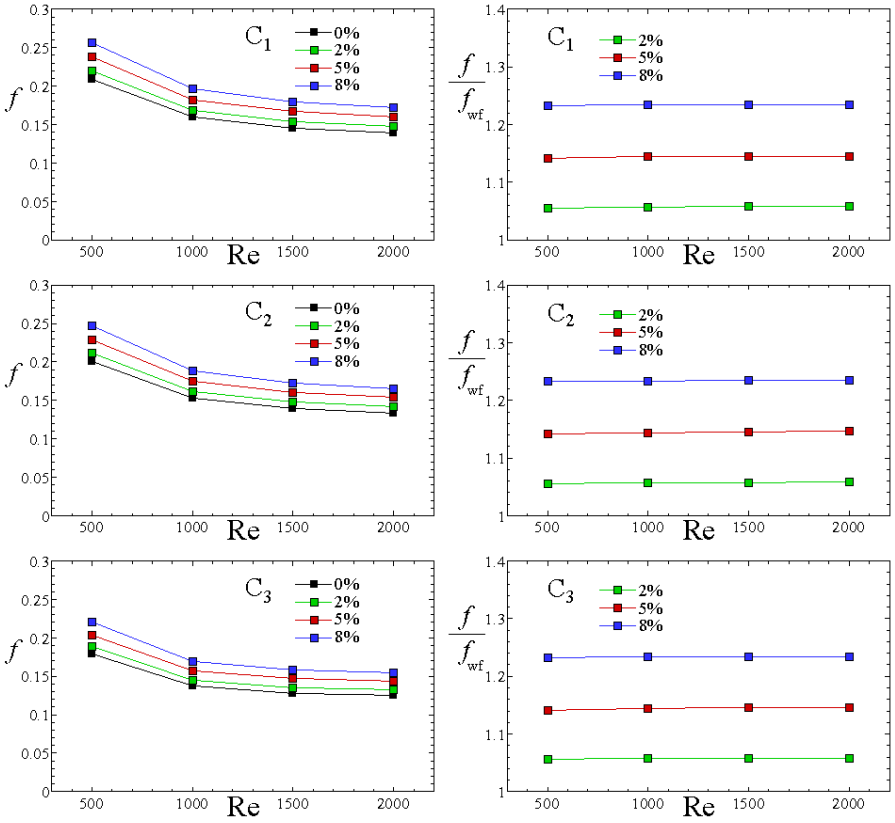

Figure 9. Effect of nanoparticle volume fraction on friction factor for C_1, C_2, and C_3.

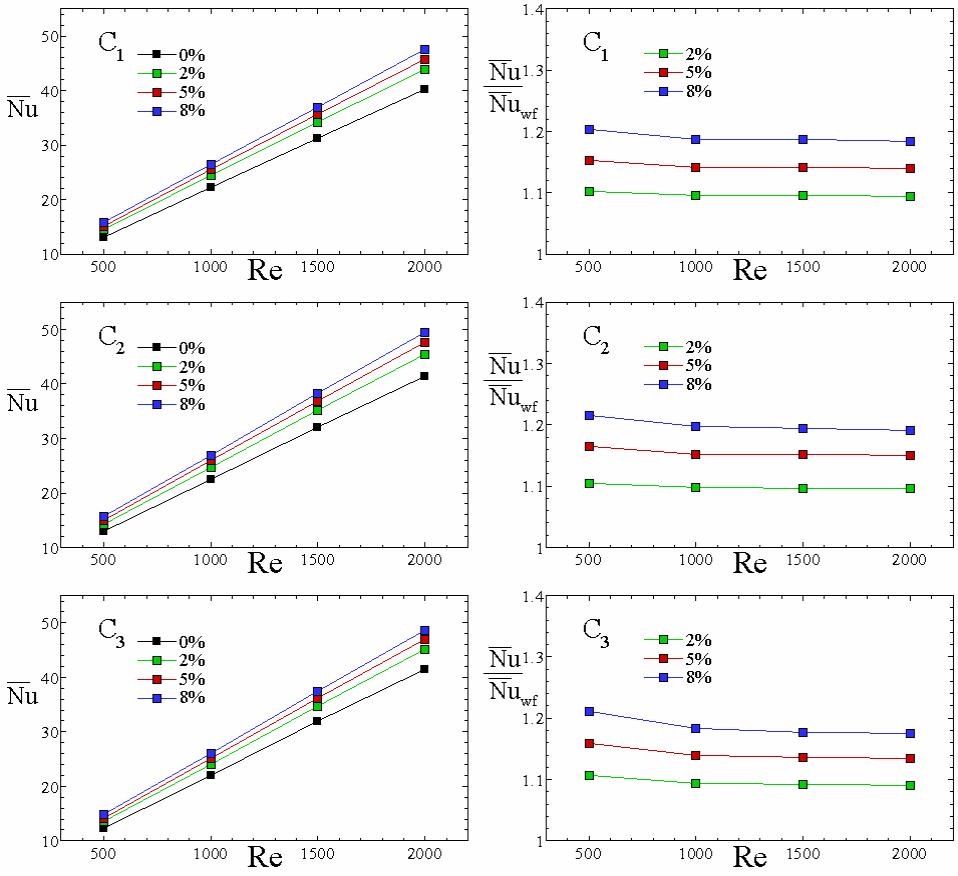

Figure 10. Effect of nanoparticle volume fraction on Nusselt number for C_1, C_2, and C_3.

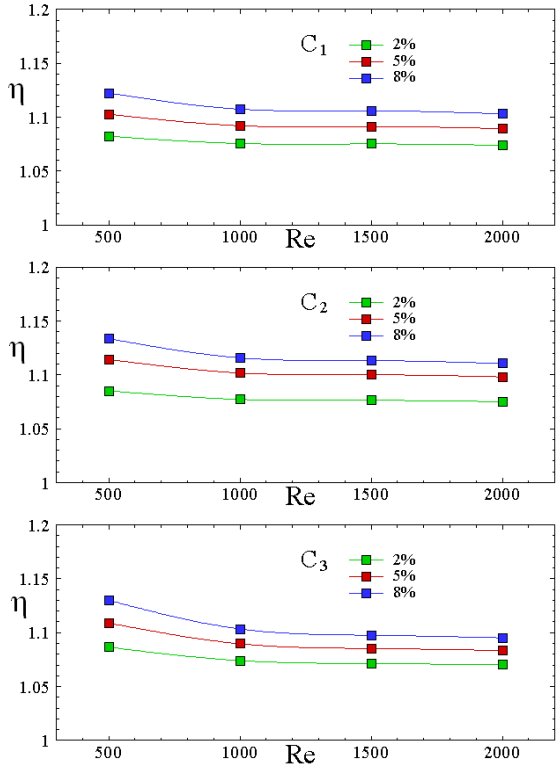

Figure 11. Variations of efficiency indices with the Reynolds number for all geometric configurations

4. CONCLUSION

In this paper, heat transfer enhancement and flow characteristics of alumina-water nanofluid through rectangular corrugated channel with different phase angles are studied numerically for a Reynolds number range of 500-2000 and nanoparticle volume fraction varying from 0 to 0.08. The governing equations are solved numerically using the finite volume method. The effects of nanoparticle volume fraction, phase angle and Reynolds number on flow behavior and heat transfer rate are presented and analyzed. It is demonstrated that corrugations develop turbulence flow, which increases flow mixing therefore enhances heat transfer. The turbulence intensity rate increases with Reynolds number and phase angle. On the other hand, heat transfer between the walls and fluid can significantly increase with addition of nanoparticles to the water. The results of the present study show that using nanofluids instead of traditional fluids can lead to further improvement in thermal performance of heat exchangers if implemented in an appropriate Reynolds number regime.

5. REFERENCES

[1]. T. Nishimura, Y. Ohori, Y. Kawamura, 1978, "Flow characteristics in a channel with symmetric wavy wall for steady flow", Journal of Chemical Engineering of Japan, 17(5), pp. 466-471.

[2]. T. Nishimura, S. Murakami, S. Arakawa, Y. Kawamura, 1990, "Flow observations and mass-transfer characteristics in symmetrical wavy-walled channels at moderate Reynolds-numbers for steady flow", International Journal of Heat and Mass Transfer, 33, pp. 835-845.

[3]. G. Wang, S.P. Vanka, 1995, "Convective heat-transfer in periodic wavy passages", International Journal of Heat and Mass Transfer, 38, pp. 3219-3230.

[4]. J.L. Goldstein, E.M. Sparrow, 1977, "Heat/mass transfer characteristics for flow in a corrugated wall channel", ASME Journal of Heat Transfer, 99, pp. 187-195.

[5]. T. Desrues, P. Marty, J. F. Fourmigue, 2012, "Numerical prediction of heat transfer and pressure drop in three-dimensional channels with alternated opposed ribs", Applied Thermal Engineering, 45-46, pp. 52-63.

[6]. S.Eiamsa-ard, P. Promvonge, 2008, "Numerical study on heat transfer of turbulent channel flow over periodic grooves", International Communications in Heat and Mass Transfer, 35, pp. 844-852.

[7]. J.Yin, G.Yang, Y. Li, 2012, "The Effects of Wavy Plate Phase Shift on Flow and Heat Transfer Characteristics in Corrugated Channel", Energy Procedia, 14, pp. 166-1573.

[8]. H. Masuda, A. Ebata, K. Teramae, N. Hishinuma, 1993, "Alteration of thermal conductivity and viscosity of liquid by dispersing ultra-fine particles(dispersions of γ-Al_2O_3, SiO_2, and TiO_2ultra-fine particles)", Netsu Bussei (Japan), 4, pp. 227-233.

[9]. U.S. Choi, 1995, "Enhancing thermal conductivity of fluids with nano-particles", ASME Fluids Engineering Division, 231, pp. 99-103.

[10]. S. U. S. Choi, Z. G. Zhang, W. Yu, F.E. Lockwood, E. A. Grulke, 2001, "Anomalous thermal conductivity enhancement in nanotube suspensions", Applied Physics Letters, 79(14), pp. 2252-2254.

[11]. Y.M. Xuan, Q. Li, 2000, "Heat transfer enhancement of nanofluids", International Journal of Heat and Fluid Flow, 21, pp. 58-64.

[12]. J.A. Eastman, U.S. Choi, S. Li, L.J. Thompson, S. Lee, 1997, "Enhanced thermal conductivity through the development of nanofluids", Nanophase and Nanocomposite Materials, 457, pp. 3-11.

[13]. A.K. Santra, S. Sen, N. Chakraborty, 2009, "Study of heat transfer due to laminar flow of copper-water nanofluid through two isothermally heated parallel plates", International Journal of Thermal Sciences, 48, pp. 391-400.

[14]. H. Heidary, M.J. Kermani, 2010, "Effect of nano-particles on forced convection in sinusoidal-wall channel", International Communications in Heat and Mass Transfer, 37, pp. 1520-1527.

[15]. M.A. Ahmed, N.H. Shuaib, M.Z. Yusoff, A.H. Al-Falahi, 2011, "Numerical investigations of flow and heat transfer enhancement in a corrugated channel using nanofluid", International Communications in Heat and Mass Transfer, 38, pp. 1368-1375.

[16]. M.A. Ahmed, N.H. Shuaib, M.Z. Yusoff, 2012, "Numerical investigations on the heat transfer enhancement in a wavy channel using nanofluid",

International Journal of Heat and Mass Transfer, 55, pp. 5891-5898.

[17]. K.V. Sharma, L. Syam Sundar, P.K. Sarma, 2009, "Estimation of heat transfer coefficient and friction factor in the transition flow with low volume concentration of Al_2O_3 nanofluid flowing in a circular tube and with twisted tape insert", International Communications in Heat and Mass Transfer, 36(5), pp. 503-507.

[18]. A. R. Darzi, M. Farhadi, K. Sedighi, S. Aallahyari, M. A. Delavar, 2013, "Turbulent heat transfer of Al_2O_3–water nanofluid inside helically corrugated tubes: Numerical study", International Communications in Heat and Mass Transfer, 41, pp. 68-75.

[19]. M. Shahi, A.H. Mahmoudi, F. Talebi, "A numerical investigation of conjugated-natural convection heat transfer enhancement of a nanofluid in an annular tube driven by inner heat generating solid cylinder", International Communications in Heat and Mass Transfer, 38(4), pp. 533-542.

[20]. S.V. Patankar, 1980, "Numerical heat transfer and fluid flow", NY: Taylor & Francis.New York.

[21]. D.C. Wilcox, 1994, "Turbulence Modeling for CFD", second ed. DCW industeries, Inc., California.

[22]. R. S. Vajjha, D. K. Das, 2009, "Experimental determination of thermal conductivity of three nanofluids and development of new correlations", International Journal of Heat and Mass Transfer, 52, pp. 4675-4682.

[23]. F.P. Incropera, D.P. DeWitt, T.L. Bergman, A.S. Lavine, 2011, "Fundamentals of heat and mass transfer", John Wiley & Sons, Inc.

[24]. R.K. Shah, A.L. London, 1978, "Laminar forced convection in ducts", academic press, New York, *San Francisco, London*